THE JOURNAL OF PHYSICAL CHEMISTRY C

Article

pubs.acs.org/JPCC

Water-Sensitive High-Frequency Molecular Vibrations in Self-Assembled Diphenylalanine Nanotubes

Xinglong Wu,*[,†,‡] Shijie Xiong,[†] Minjie Wang,[†] Jiancang Shen,[†] and Paul K. Chu*[,‡]

[†]National Laboratory of Solid State Microstructures and Department of Physics, Nanjing University, Nanjing 210093, People's Republic of China

[‡]Department of Physics and Materials Science, City University of Hong Kong, Tat Chee Avenue, Kowloon, Hong Kong, People's Republic of China

Supporting Information

ABSTRACT: High-frequency molecular vibrations in bioinspired peptide nanostructures provide insight into the important interactions between peptides and water molecules. Raman spectra acquired from diphenylalanine (FF) nanotubes show that water bonded weakly to FF molecules in the nanochannel cores leads to splitting of the molecular vibrational mode of benzene rings at 1034 cm^{-1} into a doublet with the separation diminishing with decreasing water content. X-ray diffraction discloses that loss of water results in noticeable lattice expansion in the subnanometer crystalline structure comprising hexagonal unit cells, and derivation based on the density functional theory shows that the Raman-active phonon modes often appear in pairs due to the duality of the major components in the FF molecules. Without water, the two typical peaks in the vicinity of 1034 cm^{-1} from the vibrations of two benzene rings in the FF molecule are very close and usually cannot be distinguished experimentally, but with the addition of water, the two peaks are gradually separated and the relative intensities change. Our results demonstrate that Raman scattering can be used to probe the quantity of water molecules in FF NTs via the linear dependence of the Raman mode position at the low-frequency side of the double-peak mode at 1034 cm^{-1} on water molecule number bonded to each FF molecule. This knowledge is important to the fundamental understanding of the interactions between FF nanotubes and water, device design, as well as applications to biochemistry, medicine, and molecular sensing.

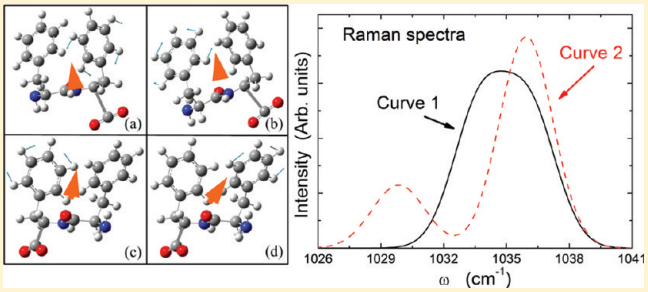

INTRODUCTION

Self-assembly of diphenylalanine (L-Phe-L-Phe, FF) molecules, the core recognition motif of the Alzheimer's disease-associated β-amyloid polypeptide, can form various stiff as well as chemically and thermally stable nanostructures in aqueous solutions including nanotubes (NTs), nanowires (NWs), nanoribbons, vertically aligned nanoforests, nanovesicles transformed from NTs, as well as well-organized films.[1−9] These self-assembled nanostructures have potential applications in biochemistry, medicine, and molecular sensing. Among the various nanostructures, FF NTs are very interesting because the formation involves hydrogen bonding, aromatic stacking, and electrostatic interactions, which can lead to different morphologies and consequently many unique and novel physical, chemical, and biological effects.[10−23] It has been shown that increasing the FF concentration in water leads to the formation of NWs, whereas decreasing the FF concentration produces NTs.[13] It has also been reported that the quantum confinement effect observed previously only from semiconductor crystals can occur in these self-assembled NTs made of biological building blocks in the form of helices with six FF molecules per turn and side chains emanating from the channel core filled with water molecules.[15−18] This implies that water molecules bonded weakly to FF molecules play an important role in the biological activity of FF NTs. The interaction between water and FF NTs is a crucial cross-disciplinary research subject encompassing biophysics, nanochemistry, and molecular sensing because it provides the platform to study new and not well-understood biological, chemical, and physical effects based on atomic-scale structural information. Hence, systematic investigation and better understanding of the interactions are crucial to device design and applications to biochemistry, biomedical engineering, and medical science.

Although Raman scattering is a useful nondestructive tool to study molecular interactions, very little work has been conducted in this area due to the complexity of FF molecular NT structures.[24] It is still unclear how addition or loss of water in the nanochannel cores affects the vibrations in FF molecules in the subnanometer scale crystalline structure (hexagonal unit cell), which shows the quantum phenomenon. In this work, we experimentally and theoretically study the Raman spectra

Received: December 14, 2011
Revised: April 9, 2012
Published: April 10, 2012

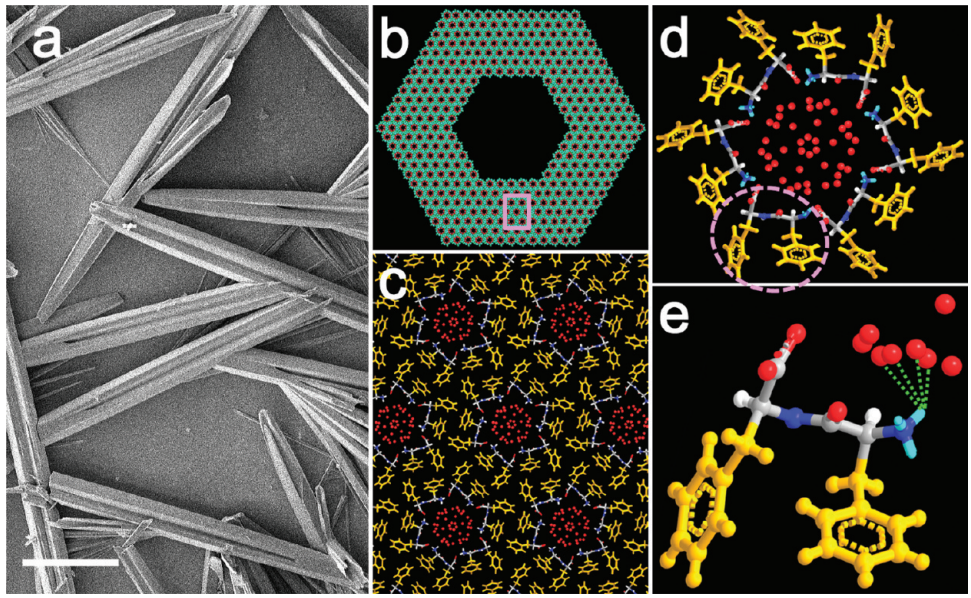

Figure 1. (a) Typical FE-SEM image of the FF MTs fabricated using a FF concentration of 90 mg/mL at an RH of 1 and 22 °C (scale bar = 10 μm). (b) Top view of the model illustrating the construction of a hexagonal FF NT. (c) Local magnification of the tube wall consisting of a large number of nanochannel cores. (d) Schematic of a highly ordered hexagonal crystalline unit cell weakly bonded to water molecules (red balls). (e) FF molecule in the nanochannel core bonded to several water molecules via intermolecular hydrogen bonds (green dotted lines).

acquired from hierarchical hexagonal FF NTs and demonstrate that water molecules bonded weakly to FF molecules in the channel cores of the NTs cause significant peak splitting and intensity change. Our results suggest that Raman scattering can be used to determine the number of water molecules in the FF NTs by probing the interaction between water and FF molecules.

EXPERIMENTAL SECTION

The water-sensitive FF NTs were prepared by evaporating a drop of fresh FF solution dissolved in 1,1,1,3,3,3-hexafluoro-2-propanol on a glass substrate.[19] The initial concentrations of the FF solutions were varied between 20 and 300 mg/mL, and the water vapor pressure was controlled during fabrication by adjusting the relative humidity (RH) at 22 °C. The FF solutions were dried for 3 min, and the FF NTs produced were characterized after 30 min.

The morphology and size of the FF NTs were determined using a field-emission scanning electron microscope (FE-SEM) equipped with an energy-diffuse X-ray spectrometer (EDXS, Hitachi High-technologies Co., Japan, acceleration voltage from 1 to 15 kV). X-ray diffraction (XRD) patterns were obtained on a Rigaku 3015 with Cu Kα radiation (λ = 0.15418 nm). Raman vibration spectra were acquired on a T64000 triple Raman system at a micro-Raman backscattering geometry using the 514.5 nm line of an Ar ion laser as the excitation source, and the resolution of the spectrometer was 0.1 cm^{-1}. The diameter of the beam was 2 μm, and the power illuminating the NTs was less than 4 mW to avoid possible sample degeneration from laser heating. Each Raman spectrum was acquired from a single microtube (MT) of different NT samples for 2 min at room temperature without the polarization configuration based on an optical microscope. The acquired spectra are the same as those excited by the 488 nm line, and so the observed Raman lines do not arise from luminescence.

RESULTS AND DISCUSSION

The samples produced with different FF concentrations under different water vapor pressure have tube-like structures. Figure 1a depicts a typical FE-SEM image of the FF MTs fabricated with an FF concentration of 90 mg/mL at an RH of 1. The MTs exhibit a hierarchical hexagonal morphology, and the radial size ranges from 2 to 5 μm.[2,10,19] Our previous study has shown that the observed FF MTs stem from assembly of many FF NTs via the dipole-field mechanism.[19] Figure 1b shows the top view illustrating construction of the hexagonal tube. The MT wall is composed of a large number of nanochannel cores as shown in Figure 1c. The schematic of the hexagonal unit cell with water (red balls) bonded weakly to the FF molecules in the channel core is shown in Figure 1d.[10,18] The main interaction between the FF molecules and water is intermolecular hydrogen bond (Figure 1e, green dotted lines). Because the interaction is weak, the water molecules can be depleted easily from the channel cores by simple processes such as drying and light exposure.[20] If the FF concentration used in the NT fabrication is small, only a small amount of water is needed. However, if the FF concentration increases, the FF NTs are water deficient and the FF will need more water to be hydrated.[13] A similar phenomenon can be observed from MTs produced at different RH values but the same FF concentration as indicated by thermogravimetric analysis.[20] Hence, the water content in the channel cores can be altered by varying the FF concentration or RH during fabrication.

Figure 2a shows two complete Raman spectra obtained from the initial commercial FF powders and FF MTs produced with an FF concentration of 60 mg/mL and RH of 1. These two spectra are very similar with respect to the vibrational mode distribution. No significant new Raman modes can be observed from the NTs, indicating that the FF molecules do not undergo major structural rearrangement when they self-assemble into NTs. This is understandable because the arrangement of FF molecules into hexagonal unit cells cannot cause large changes

dx.doi.org/10.1021/jp212087h | J. Phys. Chem. C 2012, 116, 9793−9799

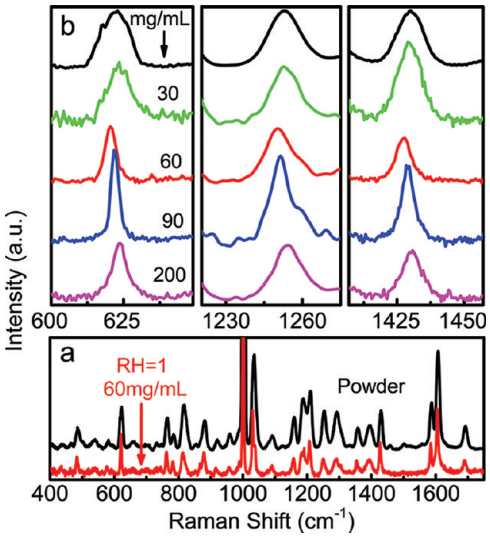

Figure 2. (a) Two complete Raman spectra acquired from the initial powders and NTs fabricated using an FF concentration of 60 mg/mL at an RH of 1. (b) Three local Raman spectra obtained from the initial powders and four NT samples fabricated with FF concentrations of 30, 60, 90, and 200 mg/mL at an RH of 1.

in the atomic structure of the FF molecules. However, the atomic vibrations in the FF molecules can be affected by the presence of weakly bonded water molecules in the channel cores. Different amounts of water molecules can significantly modify the interaction between FF molecules and consequently change the line-widths and position of the vibrational modes in the Raman spectra. Here, the NTs fabricated with different FF concentrations and RH values have different water contents as revealed by photoluminescence spectroscopy[20] and are expected to exhibit different Raman vibration behavior.

To identify the spectral differences among the MT samples, three local Raman spectra are presented in Figure 2b. They are acquired from the initial powders and four FF MT samples fabricated with FF concentrations of 30, 60, 90, and 200 mg/mL at a RH of 1. The ~623 cm^{-1} Raman peak corresponds to the vibration of the phenyl group, which is insensitive to the excitation laser polarization.[24,25] The ~1249 cm^{-1} peak is attributed to the amide III band, which is a highly coupled vibration with a strong contribution from C−N stretching. The ~1429 cm^{-1} peak is associated with CH bond deformation and depends strongly on the incident laser polarization.[24] For the powders and 30 mg/mL sample, the peak position and line-width are almost identical, indicating that the FF molecules in the two samples have similar random aggregation. FE-SEM indicates that the NTs are formed only when the FF concentration exceeds 60 mg/mL, and thus no NTs can be observed from the 30 mg/mL sample.[19] As the FF concentration is increased, the characteristic Raman peaks become narrower, and the peak positions downshift initially and then upshift gradually. When the FF concentration reaches 200 mg/mL, the peak position is almost the same as that of the 30 mg/mL sample. At the same time, the peak is wider than that of the 90 mg/mL NTs but still narrower than that of the 30 mg/mL sample. The wide peak observed from the 30 mg/mL sample is actually composed of two subpeaks with the separation determined by the interaction between water and FF molecules via hydrogen bonding, because the main difference between the NTs fabricated with different FF concentrations is the water content.

These three Raman peaks have different origins but demonstrate similar behavior with different FF concentrations and RH modification. To further investigate the peak shift, we focus on the strongest Raman peaks in the wavenumber range of 970−1060 cm^{-1} originating from the vibration of the phenyl group without a dependence on incident beam polarization. Figure 3a depicts the corresponding Raman spectra from five

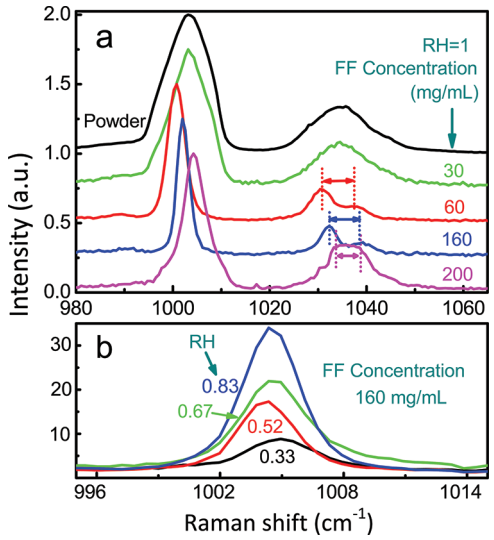

Figure 3. (a) Local Raman spectra in the range of 970−1060 cm^{-1} acquired from the four NT samples synthesized with FF concentrations of 30, 60, 90, and 200 mg/mL at an RH of 1. Splitting of the Raman peak on the high-energy side can be observed clearly. (b) Local Raman spectra in the range of 1002−1012 cm^{-1} acquired from the four NT samples fabricated with an FF concentration of 160 mg/mL at RH values of 0.33, 0.52, 0.67, and 0.83.

MT samples. It is clear that the change in the position and width of the ~1005 cm^{-1} peak, which belongs to the aromatic ring breathing mode,[24] is consistent with that shown in Figure 2b. Interestingly, the ~1034 cm^{-1} mode of the 30 mg/mL sample manifests as a single broad peak, but that of the 60 mg/mL MTs clearly splits into two subpeaks at 1031.2 and 1038.4 cm^{-1} with a separation of 7.2 cm^{-1}. The two subpeaks upshift, and the separation decreases to 6.6 cm^{-1} as observed from the 90 mg/mL NTs. Here, it should be noted that the high-frequency peak has a relatively low intensity in the two samples. Finally, in the 200 mg/mL NT sample, the two subpeaks seemingly merge into one peak again with the line-width larger than that of each subpeak. The wide peak can be Lorentzian divided into two subpeaks (their positions are marked by the vertical dotted lines). The upshift of the high-frequency subpeak is slightly smaller than that of the low-frequency one. Their separation becomes 4.7 cm^{-1}. It is apparently due to more water deficiency, and so the Raman peaks are separated less. As the FF concentration is further increased, the 1034 cm^{-1} mode still shows a single peak structure but becomes slightly broader. By deconvoluting the broad peak into two subpeaks, the low-frequency peak begins to exhibit a slight downshift. The feature and behavior of the 1034 cm^{-1} Raman peak are very similar to those of the 623, 1005, 1249, and 1429 cm^{-1} peaks in which the high-frequency peak has a low intensity so that it cannot be detected. The line-width changes

dx.doi.org/10.1021/jp212087h | J. Phys. Chem. C 2012, 116, 9793−9799

are also noticeable from spectra acquired from NTs fabricated using the same FF concentration but different RH values, as shown in Figure 3b. As the RH value drops, the line-width of the Raman peak at ~1005 cm^{-1} decreases gradually, further corroborating the decreased interactions between water and FF molecules.

The reduced interactions caused by loss of the water lead to lattice expansion in the hexagonal nanocrystalline unit cell structure (Figure 1d). To study this effect, the XRD patterns of the FF NTs fabricated with different FF concentrations or different RH values are analyzed. Figure 4a shows two complete

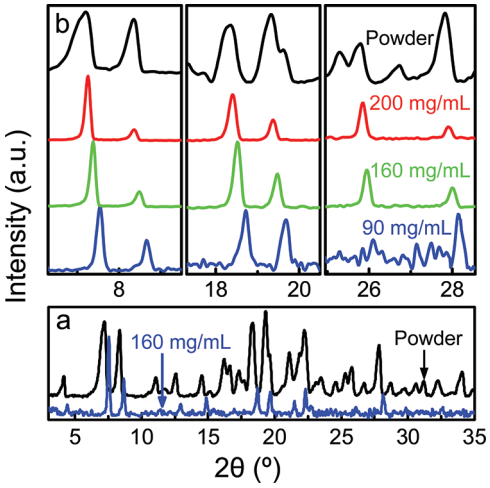

Figure 4. (a) Two complete XRD patterns acquired from the initial powders and NTs fabricated with an FF concentration of 160 mg/mL at an RH of 1. (b) Three local XRD patterns acquired from the initial powders and three FF NT samples produced with FF concentrations of 90, 160, and 200 mg/mL at a RH of 1.

XRD patterns acquired from the initial powders and NTs fabricated using an FF concentration of 160 mg/mL at an RH of 1. Some diffraction peaks disappear, and the other diffraction peaks observed from the 160 mg/mL NTs are narrower than those from the powders. This implies that the FF molecules are not disorderly aggregated in the NT samples, but rather an orderly arrangement is apparent. Figure 4b depicts three local XRD patterns obtained from the 200, 160, and 90 mg/mL NTs produced at an RH of 1. These diffraction peaks can be indexed to the nanocrystalline unit cell structure of FF molecules.[13,18] Although the diffraction peak shifts are not linear with increasing FF concentrations (decreasing water contents), all of the XRD peaks shift toward the low 2θ side. Simple calculation shows that the expansion of the water-deficient channel in the plane perpendicular to the channel of the 90–200 mg/mL samples is 4.2%, whereas the aromatic stacking distance along the channel contracts by less than 0.07%.[13] Hence, hydrogen bonds are dominant, and the XRD results also indicate that the diffraction peak shift is not due to random aggregation of FF molecules because no distinct peak broadening can be observed as compared to the initial powders. With regard to the NT samples produced with an FF concentration of 160 mg/mL at RH values of 0.33, 0.52, and 0.83, XRD also reveals that with decreasing RH, the diffraction peaks shift toward the low 2θ side,[20] and this is consistent with Figure 4. Therefore, even though the water molecules are weakly bonded to the FF molecules in the nanochannel cores, they play an essential role in the vibrational characteristic modification of the FF molecules.

It should be stressed that changes in the aromatic stacking distance may not be responsible for the observed Raman behavior because the distance change is relatively small as shown by XRD. A previous report also confirms this.[13] To further investigate this phenomenon, the 120 mg/mL FF NT sample is divided into two pieces. The first piece is used as is (sample 1), whereas the second piece is dried at 90 °C for 16 h (sample 2) and then exposed to saturated water vapor at 90 °C for 16 h (sample 3). The NTs after post-treatment possess the same morphology, and the Raman spectra show features similar to those in Figure 3a. The Fourier transform infrared spectra of the three samples in the wavenumber range of 400–4000 cm^{-1} do not reveal chemical bonding changes with the exception of intensity changes in the vibration bands associated with water molecules at ~3400 cm^{-1}.[20] Hence, the results further reveal that the spectral modification stems from the modified interactions between water and FF molecules. Here, it should be mentioned that because water molecules are hydrogen-bonded to the FF molecules in the channel cores, the same postprocessing conducted on different NT samples (drying or exposure to saturated water vapor) cannot ensure the same and reproducible water addition and loss.[20] Therefore, the Raman spectra of the NT samples after different postprocessing may show different peak widths and positions depending on the amount of water interacting with the FF molecules. Here, it should be emphasized that these FF NTs are not intended to be water sensors in the conventional sense, although they are able to detect water in air or other media. Instead, our results demonstrate that Raman spectra obtained from the NTs can be used to probe the amount of water molecules bonded to the FF molecules. This is important because water molecules play an important role in the biological properties of FF PNTs.

To obtain further insight, the vibrational characteristics of the FF NT systems and the effects of water molecules are studied by density functional theory (DFT) calculation using the Perdew–Burke–Ernzerhof potential function and Gaussian 03 code.[26,27] Because the vibrational modes are usually located within a specific part of the system, all of the Raman active modes in the FF molecule are calculated. Geometric optimization is performed by the density functional method by adopting the frozen-core approximation.[28,29] Calculations of the phonon frequencies and Raman intensities are based on the numerical differentiation of energies from the DFT results,[30,31] and the effect of water molecules is calculated using the polarized continuum model (PCM).[32] The calculation results show that the typical phonon modes in the range of 1030–1040 cm^{-1} shown in Figure 3a correspond to the in-plane stretching–shrinking oscillations of the benzene rings, as shown in Figure 5a and b. Because there are two nearly identical benzene rings in a FF molecule, two such modes are located on different benzene rings. In the absence of water, the calculated frequencies of the two modes (ω_1 = 1033.73 cm^{-1} and ω_2 = 1036.12 cm^{-1}) are very close, and their Raman activities are also almost the same (A_1 = 2.3227 and A_2 = 2.2755). That is, the two benzene rings in the FF molecule are almost the same, and coupling between the two modes is weak (localized behavior). Consequently, peak splitting is difficult to observe by experiments. This corresponds to the case observed from the 200 mg/mL NT sample in which only a broad peak is detected. However, in the presence of the weakly bonded water molecules, the calculated frequencies of the two modes become

dx.doi.org/10.1021/jp212087h | J. Phys. Chem. C 2012, 116, 9793–9799

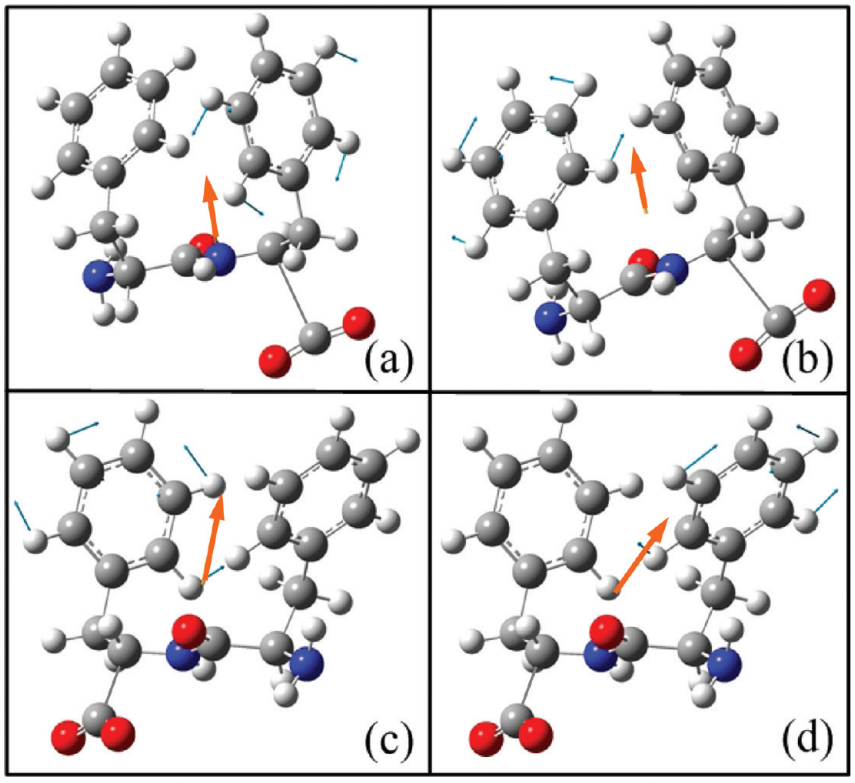

Figure 5. (a–d) Displacement vectors of atoms (blue arrows) and dipole derivative unit vectors (yellow arrows) for modes ω_1 (a and c) and ω_2 (b and d) of an FF molecule without water (a and b) and with water (c and d).

ω_1 = 1029.85 cm^{-1} and ω_2 = 1035.94 cm^{-1} with Raman activities A_1 = 13.8953 and A_2 = 45.7743, respectively. The corresponding oscillations of the two benzene rings are shown in Figure 5c and d. The two peaks are separated in the presence of water, and their Raman activities are significantly different, as in the case of the 1034 cm^{-1} mode observed from the 60 and 160 mg/mL NT samples (Figure 3a). The increased separation is due to the strengthened coupling between the two modes in the presence of water, whereas the difference in the Raman activity originates from the variation of the dipole derivative direction (yellow arrow) as a result of water molecule polarization. Without water, the dipole derivative directions are along the same straight line, but with water molecules, they are along different lines as shown in Figure 5a–d. This variation in the dipole derivative directions depends on the amount of water molecules in the channel cores. Considering the broadening of the Raman peaks, Figure 6 plots the Raman spectra without water (curve 1) and with water (curve 2) of the Raman peaks. Obviously, if there are different water amounts in the NTs, A_1, A_2, ω_1, ω_2, and $\Delta\omega = \omega_2 - \omega_1$ all will be different. When the dipole derivation directions of the two benzene rings interacting with water molecules are perpendicular to each other, A_1 or A_2 will become extremely small. Consequently, the subpeak disappears, as illustrated by the Raman modes at 623, 1005, 1249, and 1429 cm^{-1} in Figures 2b and 3a. The curves in Figure 6 clearly explain the shifting, splitting, and relative intensity modification of the observed Raman modes for different water contents. The dual structure in the FF molecules can produce similar pairing features in other modes located on the benzene rings or other parts of the molecules.

To determine the quantity of water molecules bonded to each FF molecule by Raman spectroscopy via the interaction between water and FF molecules, the influence of water

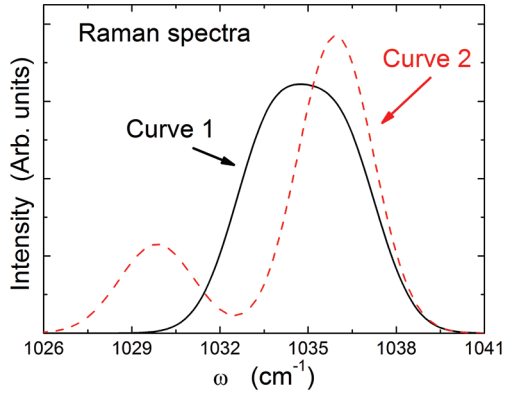

Figure 6. Raman spectra obtained from modes ω_1 and ω_2. The solid black and dashed red lines correspond to the results calculated by Gaussian 03 without and with water molecules, respectively.

molecules on the characteristic vibration mode in the wavelength range of 1020–1050 cm^{-1} is quantitatively calculated. As there are no rigid contacts between the FF and water molecules, the coupling between them mainly comes from the long-range electric interaction. The field at an atom n in the FF molecule produced by dipoles of relevant N water molecules is:[33]

$$\vec{E}_n = \frac{1}{4\pi\varepsilon_0}\sum_{j=1}^{N}\frac{3\vec{\mu}_j\cdot\vec{R}_{nj}\vec{R}_{nj} - \vec{\mu}_j R_{nj}^2}{R_{nj}^5}$$

where $\vec{\mu}_j$ is the dipole of the jth water molecule, $\vec{R}_{nj}$ is the distance between n and j, and ε_0 is the dielectric constant. When the jth water molecule vibrates at mode ω_0 with generalized displacement X_j and the FF molecule vibrates at

dx.doi.org/10.1021/jp212087h | J. Phys. Chem. C 2012, 116, 9793–9799

mode ω_i (i = 1, 2) with generalized displacement x_i, the coupling of modes ω_1 and ω_2 in the FF molecule with mode ω_0 of water molecules can be described by the energy change $\Delta E = (1/2)\sum_{i=1}^{2}\sum_{j=1}^{N}\lambda_{ij}^2 x_i X_j$ to the lowest order of the displacements. Here, the coupling strength is

$$\lambda_{ij}^2 = \frac{1}{2\pi\varepsilon_0}\sum_n \frac{3(\vec{\mu}_{0j}\cdot\vec{R}_{nj})(\vec{\eta}_{in}\cdot\vec{R}_{nj}) - R_{nj}^2(\vec{\mu}_{0j}\cdot\vec{\eta}_{in})}{R_{nj}^5}$$

where $\vec{\mu}_{0j}$ and $\vec{\eta}_{in}$ are defined as $\Delta\vec{\mu}_j = \vec{\mu}_{0j}X_j$ and $\Delta\vec{R}_n = \sum_{i=1}^{2}\vec{\eta}_{in}x_i$. Because the positions and dipole orientations of water molecules are spread, the values of λ_{ij}^2 fluctuate. By using the perturbation theory, the frequency shifts of ω_1 and ω_2 due to coupling to water molecules can be calculated as $\delta\omega_i = -\alpha_i N$ for i = 1 and 2, where $\alpha_i = (\langle\lambda_{ij}^4\rangle)/(2\omega_i(\omega_0^2 - \omega_i^2))$ with $\langle\lambda_{ij}^4\rangle$ denoting the averaging over N water molecules for λ_{ij}^4. In the calculation, we only consider the bending mode of ω_0 = 1767 cm^{-1} for the water vibrations, because it is mostly close to ω_1 and ω_2 among the three H_2O modes[34] and thus interacts most strongly with ω_1 and ω_2. Frequency ω_1 as a function of the number of water molecules attached to each FF molecule can also be calculated directly from vibrational equations with randomly distributed coupling strengths, yielding the results in Figure 7. The dependence of ω_1 on the molecule number N can

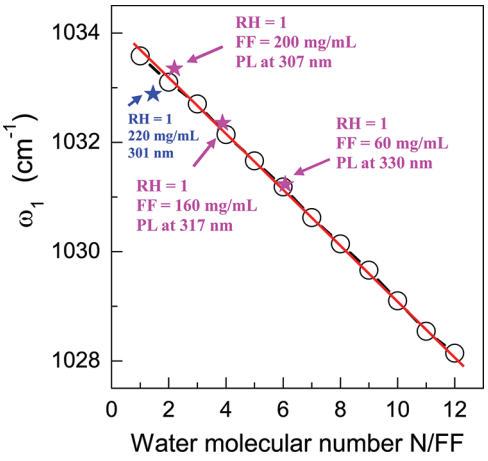

Figure 7. Frequency ω_1 as a function of number of water molecules attached to each FF molecule in a nanochannel core. The linear fitting is obtained with α_1 = 0.5 cm^{-1}. The points labeled "★" are the experimental data.

be fitted linearly by setting parameter α_1 = 0.5 cm^{-1}. This interesting result suggests that we can use the frequency of the Raman spectrum to measure the density of water molecules in the FF NT. To corroborate the validity of the theoretical derivation, the photoluminescence spectra of the three FF NT samples fabricated with FF concentrations of 60, 160, and 200, 220 mg/mL at RH = 1 are obtained, and the mean water molecule numbers N coupled to each FF molecule are derived from the thermogravimetric analysis. We have observed a correlation between the PL peak position and water number N coupled to each FF molecule based on the thermogravimetric results.[20] If the NT diameter and length are known, we can derive the water molecule numbers in the NT based on a biological building block cell. These building block cells are regularly arranged in the tube walls and have a similar subnanometer scale for the two sidewalls $a = b$ = 2.407 nm and c = 0.545 nm as reported by Gorbitz.[10] At the same time, the ω_1 value can be obtained from Figure 3a. Finally, we provide the four experimental data points (N, ω_1) in Figure 7 (labeled with ★). The three points obtained from the 60, 160, and 200 mg/mL NT samples agree very well with the theoretical curve, but the experimental point from the 220 mg/ML NT sample has a large deviation from the calculated result. This indicates that when the FF concentration exceeds 220 mg/mL or the amount of water amount is below a certain value, the theoretical calculation cannot predict the number of water molecules in the NTs. This theoretical deviation is based on the assumption of noninteractions between the benzene rings in the nanochannel direction and in the plane perpendicular to nanochannel. In this case, these interactions are weak and can be neglected. When there are no water molecules, these interactions will be dominant and need to be considered in the theoretical calculation. However, under the current experimental conditions with FF concentrations lower than 200 mg/mL, our results provide strong evidence that Raman scattering can be used effectively to detect the number of water molecules in nanostructured FF materials. Because FF nanomaterials generally consist of the self-assembled peptide quantum dots on the subnanometer scale,[14,15] we believe that the Raman spectral features induced by the interaction between water and FF molecules will not be affected by the types of nanomaterials.

CONCLUSION

Water bonded weakly to FF molecules in the nanochannel cores gives rise to splitting of the molecular vibrational mode into a doublet, and the absolute separation decreases with lower water content. The separation decreases as water is lost, finally yielding a single peak structure. XRD reveals that water deficiency leads to lattice expansion in the hexagonal nanocrystalline unit cell structure as a result of the reduced interactions between water and FF molecules. DFT calculation discloses that the dual structure of the FF molecules produces the double phonon modes. The separation and relative intensity of the two subpeaks depend on the amount of water molecules in the channel cores of the FF NTs. Our experimental and theoretical results clearly demonstrate that Raman scattering can be used to characterize the interactions between FF molecules and water and especially to determine the water molecule number in the self-assembled FF NTs.

ASSOCIATED CONTENT

Supporting Information

Complete author list of ref 25. This material is available free of charge via the Internet at http://pubs.acs.org.

AUTHOR INFORMATION

Corresponding Author

*Tel.: 86-25-83686303 (X.L.W.), 852-34427724 (P.K.C.). Fax: 86-25-83595535 (X.L.W.), 852-34420542 (P.K.C.). E-mail: hkxlwu@nju.edu.cn (X.L.W.), paul.chu@cityu.edu.hk (P.K.C.).

Notes

The authors declare no competing financial interest.

ACKNOWLEDGMENTS

This work was supported by the National Basic Research Programs of China under Grant No. 2011CB922102. Partial support was also from the PAPD, National Natural Science Foundations (Nos. 60976063 and 10874071), Hong Kong

Research Grants Council (RGC) General Research Grants (GRF) CityU 112510, and City University of Hong Kong Strategic Research Grant (SRG) No. 7008009.

REFERENCES

(1) Reches, M.; Gazit, E. *Science* **2003**, *300*, 625−627.
(2) Reches, M.; Gazit, E. *Nat. Nanotechnol.* **2006**, *1*, 195−200.
(3) Hendler, N.; Sidelman, N.; Reches, M.; Gazit, E.; Rosenberg, Y.; Richter, S. *Adv. Mater.* **2007**, *19*, 1485−1488.
(4) Ryu, J.; Park, C. B. *Adv. Mater.* **2008**, *20*, 3754−3758.
(5) Han, T. H.; Oh, J. K.; Park, J. S.; Kwon, S.-H.; Kim, S.-W.; Kim, S. O. *J. Mater. Chem.* **2009**, *19*, 3512.
(6) Yan, X.; Cui, Y.; He, Q.; Wang, K.; Li, J.; Mu, W.; Wang, B.; Ouyang, Z. *Chem.-Eur. J.* **2008**, *14*, 5974−5980.
(7) Yan, X.; He, Q.; Wang, K.; Duan, L.; Cui, Y.; Li, J. *Angew. Chem.* **2007**, *119*, 2483−2486.
(8) Yan, X.; He, Q.; Wang, K.; Duan, L.; Li, J. *Angew. Chem., Int. Ed.* **2007**, *46*, 2431−2434.
(9) Bose, P. P.; Das, A. K.; Hegde, R. P.; Shamala, N.; Banerjee, A. *Chem. Mater.* **2007**, *19*, 6150−6157.
(10) Gorbitz, C. H. *Chem.-Eur. J.* **2001**, *7*, 5153−5159.
(11) Makin, O. S.; Atkins, E.; Sikorski, P.; Johansson, J.; Serpell, L. C. *Proc. Natl. Acad. Sci. U.S.A.* **2005**, *102*, 315−320.
(12) Gazit, E. *FEBS J.* **2005**, *272*, 5971−5978.
(13) Kim, J. B.; Han, T. H.; Kim, Y. I.; Park, J. S.; Choi, J.; Churchill, D. G.; Kim, S. O.; Ihee, H. *Adv. Mater.* **2010**, *22*, 583−587.
(14) Amdursky, N.; Molotskii, M.; Aronov, D.; Adler-Abramovich, L.; Gazit, E.; Rosenman, G. *Nano Lett.* **2009**, *9*, 3111−3115.
(15) Amdursky, N.; Molotskii, M.; Gazit, E.; Rosenman, G. *Appl. Phys. Lett.* **2009**, *94*, 261907.
(16) Amdursky, N.; Gazit, E.; Rosenman, G. *Adv. Mater.* **2010**, *22*, 2311−2315.
(17) Ryu, J. K.; Lim, S. Y.; Park, C. B. *Adv. Mater.* **2009**, *21*, 1577−1581.
(18) Gorbitz, C. H. *Chem. Commun.* **2006**, 2332−2334.
(19) Wang, M. J.; Du, L. J.; Wu, X. L.; Xiong, S. J.; Chu, P. K. *ACS Nano* **2011**, *5*, 4448−4454.
(20) Wang, M. J.; Xiong, S. J.; Wu, X. L.; Chu, P. K. *Small* **2011**, *7*, 2801−2807.
(21) Amdursky, N.; Beker, P.; Shklovsky, J.; Gazit, E.; Rosenman, G. *Ferroelectrics* **2010**, *399*, 107−117.
(22) Rosenman, G.; Beker, P.; Koren, I.; Yevnin, M.; Bank, B.; Mishina, E.; Semin, S. *J. Pept. Sci.* **2011**, *17*, 75−87.
(23) Amdursky, N.; Beker, P.; Koren, I.; Bank-Srour, B.; Mishina, E.; Semin, S.; Rasing, T.; Rosenberg, Y.; Barkay, Z.; Gazit, E.; Rosenman, G. *Biomacromolecules* **2011**, *12*, 1349−1354.
(24) Lekprasert, B.; Sedman, V.; Roberts, C. J.; Tedler, S. J. B.; Notingher, I. *Opt. Lett.* **2010**, *35*, 4193−4195.
(25) Tuma, R. *J. Raman Spectrosc.* **2005**, *36*, 307−319.
(26) Frisch, M. J.; Trucks, G. W.; Schlegel, H. B.; Scuseria, G. E.; Robb, M. A.; Cheeseman, J. R.; Zakrzewski, V. G.; Montgomery, J. A., Jr.; Stratmann, R. E.; Burant, J. C.; et al. *Gaussian 03*, revision A.1; Gaussian, Inc.: Pittsburgh, PA, 2003. (See the complete author list in the Supporting Information.)
(27) Perdew, J. P.; Burke, K.; Ernzerhof, M. *Phys. Rev. Lett.* **1996**, *77*, 3865−3868.
(28) Foresman, J. B.; Head-Gordon, M.; Pople, J. A.; Frisch, M. J. *J. Phys. Chem.* **1992**, *96*, 135−149.
(29) Peng, C.; Ayala, P. Y.; Schlegel, H. B.; Frisch, M. J. *J. Comput. Chem.* **1996**, *17*, 49−56.
(30) Krishnan, R.; Schlegel, H. B.; Pople, J. A. *J. Chem. Phys.* **1980**, *72*, 4654−4655.
(31) Kormornicki, A.; Jaffe, R. L. *J. Chem. Phys.* **1979**, *71*, 2150−2160.
(32) Cossi, M.; Scalmani, G.; Rega, N.; Barone, V. *J. Chem. Phys.* **2002**, *117*, 43−54.
(33) Kapitan, J.; Dracinsky, M.; Kaminsky, J.; Benda, L.; Bour, P. *J. Phys. Chem. B* **2010**, *114*, 3574−3582.
(34) Wilson, E. B.; Decius, J. C.; Cross, P. C. *Molecular Vibrations*; McGraw-Hill: New York, 1955.